

ARTICLES

Weak Correlations between Local Density and Dynamics near the Glass Transition[†]J. C. Conrad,[‡] F. W. Starr,[§] and D. A. Weitz^{*,‡}*Department of Physics and DEAS, Harvard University, 29 Oxford St, Cambridge, Massachusetts 02138, and Department of Physics, Wesleyan University, Middletown, Connecticut 06457**Received: March 17, 2005; In Final Form: May 12, 2005*

We perform experiments on two different dense colloidal suspensions with confocal microscopy to probe the relationship between local structure and dynamics near the glass transition. We calculate the Voronoi volume for our particles and show that this quantity is not a universal probe of glassy structure for all colloidal suspensions. We correlate the Voronoi volume to displacement and find that these quantities are only weakly correlated. We observe qualitatively similar results in a simulation of a polymer melt. These results suggest that the Voronoi volume does not predict dynamical behavior in experimental colloidal suspensions; a purely structural approach based on local single particle volume likely cannot describe the colloidal glass transition.

1. Introduction

Glasses are dense materials that behave mechanically like solids but are structurally indistinguishable from liquids. The fundamental mechanism for the glass transition is not well-understood; as a liquid is cooled into a glass, its viscosity increases by many orders of magnitude, yet its static structure factor changes almost imperceptibly. One conceptual approach to the glass transition, which attempts to connect glassy structure to dynamics, relates the increase in viscosity as the liquid is cooled to the decrease in “free volume” available to the liquid’s constituent molecules.^{1–4} Free volume concepts have not been rigorously tested because few methods exist to directly measure or compute free volume. Instead, attempts to test free volume approaches have used an alternate, rigorously defined measure of local volume, the Voronoi volume, v , defined as the volume of space closer to a particular particle center than to any other.⁵ Curiously, simulations suggest that the distribution of Voronoi volume, $P(v)$, is universal for liquids.⁶ The existence of regular liquid structure supports structural approaches to the glass transition that include packing effects arising from hard-core repulsion.^{7–9} Additional simulations suggest that v may be correlated to local dynamical fluctuations;^{5,10–13} these simulation results also suggest a connection between the Voronoi volume and glassy dynamics. Unfortunately, free volume ideas have not been thoroughly tested in experiments, because traditional techniques for studying glasses average over many particles and cannot access information on the scale of a single molecule. An experimental probe of these ideas would elucidate the connection between local dynamics and local structure in systems near the glass transition.

In this paper, we probe the relationship between local structure, characterized by Voronoi volume, and local dynamics,

characterized by particle displacements. We show that the Voronoi volume is not a universal probe of glassy structure and that v is only weakly correlated to a particle’s displacement. As a model system, we use dense colloidal suspensions which undergo a glass transition as the volume fraction, ϕ , is increased above $\phi_g \sim 0.58$; this makes them an excellent system in which to experimentally measure the correlation between the local volume of a particle and its dynamics. We image fluorescently labeled colloidal particles with confocal microscopy.^{14–17} We calculate the distribution of Voronoi volumes for two different colloidal suspensions and find that the distribution is universal for a suspension with a harder interparticle potential and not universal for a suspension with a softer interparticle potential. In each type of suspension, we correlate the Voronoi volume of a particle to its displacement and find that these quantities are only weakly correlated; computer simulations of a glass-forming polymer melt exhibit the same behavior. These results suggest that v does not predict dynamical behavior in dense colloidal suspensions.

2. Experimental System and Procedure

We study two different types of dense suspensions of poly-(methyl methacrylate) spheres, sterically stabilized by poly-12-hydroxystearic acid.²² The colloids in the first preparation are fluorescently labeled with nitrobenzoxazole (NBD) during the colloid synthesis. To minimize sedimentation and scattering, the colloids are suspended in a three-component mixture of distilled cyclohexyl bromide, anhydrous decahydronaphthalene, and anhydrous tetrahydronaphthalene, which closely matches both the particle density $\rho \approx 1.225$ g/mL and index of refraction $n \approx 1.50$. The average colloid radius is 914 nm, and the polydispersity in radius is roughly 7% of the mean. The colloids in the second preparation are fluorescently labeled with rhodamine 6G perchlorate after the colloid synthesis and are suspended in a mixture of cycloheptyl bromide and decahydronaphthalene. The average colloid radius is 1.18 μm , and the polydispersity in radius is roughly 5% of the mean. The data for the second

[†] Part of the special issue “Irwin Oppenheim Festschrift”.

^{*} To whom correspondence should be addressed. E-mail: weitz@deas.harvard.edu.

[‡] Harvard University.

[§] Wesleyan University.

preparation are taken from refs 15 and 18. Optical tweezer measurements of the two-particle pair distribution function, $g(r)$, suggest that the potential of the second system is very slightly softer than that of the first system.

For all experiments, the samples are stirred for several minutes for about 1 h before each experiment, which randomizes the particle positions and initializes the samples into a state with no long-range correlations.^{15,16} We image the particles in three dimensions using confocal microscopy and locate their centers to within $0.03 \mu\text{m}$ in the horizontal plane and $0.05 \mu\text{m}$ in the vertical plane.^{15,17} We then follow the time evolution of a $33 \mu\text{m} \times 35 \mu\text{m} \times 20 \mu\text{m}$ section of the suspension for the first preparation and a $69 \mu\text{m} \times 64 \mu\text{m} \times 14 \mu\text{m}$ section of the suspension for the second preparation; we follow the time evolution of the particle motions for up to 12 h. Using software, we track the positions of roughly 4000 particles over the duration of the experiment.²³

We determine the volume fraction, ϕ , directly from the confocal images. We first characterize the size of the colloids using confocal microscopy. We measure the diffusion coefficient, D_0 , by tracking particles in dilute suspension and computing the mean-square displacement; we then calculate the particle radius, a , using the Stokes–Einstein relation, $a = k_B T / 6\pi\eta D_0$. We calculate the Voronoi volume for every particle in each suspension by identifying every particle's nearest neighbors, calculating the midpoints of the nearest-neighbor bonds, and constructing the Voronoi polyhedra.²⁴ We then compute the average Voronoi volume for each suspension, $\langle v \rangle$, and calculate $\phi = v_0 / \langle v \rangle$. The volume fraction obtained has a systematic bias due to errors associated with the measurement of the particle radius; however, the relative volume fractions within each suspension are correct.

3. Experimental Results

To test whether the scaling seen in simulations is also seen in experiments, we calculate the distribution of Voronoi volumes, v , for our suspensions and scale by the standard deviation, σ_v .⁶ We plot the normalized distributions of Voronoi volume, $\sigma_v P(v)$, as a function of the normalized Voronoi volume, $(v - \langle v \rangle) / \sigma_v$, for samples of the harder-potential preparation with $0.34 \leq \phi \leq 0.58$ in Figure 1a. The scaled distributions fall onto a universal curve over a wide range of ϕ in the supercooled liquid, in excellent agreement with the simulation results.⁶ The standard deviation, σ_v , decreases from 1.15 at $\phi = 0.34$ to 0.71 at $\phi = 0.52$ and then increases slightly to 0.73 at $\phi = 0.58$. In contrast, for softer-potential colloidal suspensions with $0.46 \leq \phi \leq 0.61$, the distributions of v do not collapse onto a master curve with this scaling (Figure 1b). The scaling fails both below and above ϕ_g ; the distributions of Voronoi volumes at $\phi = 0.56$, just below ϕ_g , and at $\phi = 0.61$, above ϕ_g , are more sharply peaked than the universal curve shown in Figure 1a. The distribution of scaling factors, σ_v , is also broader for these samples. The maximum standard deviation measured, 1.25, occurs at $\phi = 0.35$, while the minimum measured σ_v is 0.92 at $\phi = 0.60$; however, σ_v does not exhibit a marked trend with increasing ϕ . By this measure of static structure, the structures of the two different colloidal preparations are different. Measurements of $g(r)$ at these ϕ confirm this difference; the nearest-neighbor peak heights are greater for samples with a softer potential, as shown in Figure 2. This sharpness may also reflect the smaller polydispersity of these samples. This result suggests that a relatively sharp core interaction is needed to obtain universal behavior of $P(v)$.

To test the correlation between local structure and dynamics, we first characterize the dynamics of the suspensions by

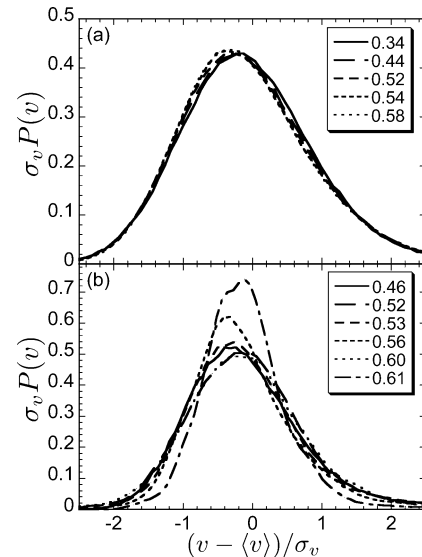


Figure 1. Scaled Voronoi volume histograms, $\sigma_v P(v)$, for two different colloidal potentials, as a function of the normalized Voronoi volume, $(v - \langle v \rangle) / \sigma_v$, for (a) colloidal samples with harder potential and (b) colloidal suspensions with softer potential. The histograms of the colloidal suspensions with a potential closer to that of hard spheres follow the scaling found in ref 6, while the histograms of the suspensions with a slightly softer potential do not.

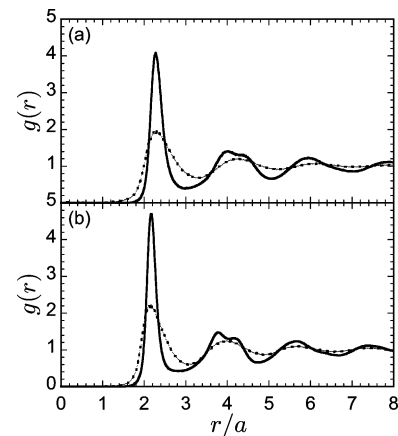


Figure 2. Pair distribution function, $g(r)$, versus normalized radius, r/a , for (a) $\phi = 0.44$ (first preparation, dotted) and $\phi = 0.46$ (second, solid) and (b) $\phi = 0.52$ (first, dotted) and $\phi = 0.52$ (second, solid).

identifying the most dynamically heterogeneous subsets. We expect the correlation between local structure and dynamics will be strongest for the particles that undergo large displacements or are frozen. We calculate the displacements of all particles over all time intervals, τ , and then identify for each τ the particles with the 10% largest and smallest displacements.^{14,15} We calculate the mean-square displacement, $\langle \Delta x^2(\tau) \rangle$, for the large- and small-displacement subsets of particles (Figures 3 and 4). For all ϕ and for all samples in both colloidal preparations, $\langle \Delta x^2(\tau) \rangle$ of the fastest 10% of the particles is roughly 1 order of magnitude larger than the sample-averaged $\langle \Delta x^2(\tau) \rangle$, whereas $\langle \Delta x^2(\tau) \rangle$ of the slowest 10% is between 2 and 3 orders of magnitude smaller. While the magnitudes of the displacements differ by many orders of magnitude, the shapes of the $\langle \Delta x^2(\tau) \rangle$ curves of the large-displacement and small-displacement particles are roughly the same as that of the sample-averaged curves. The large difference between the magnitudes of $\langle \Delta x^2(\tau) \rangle$ of the fastest and slowest particles confirms that the average dynamical behavior of these two

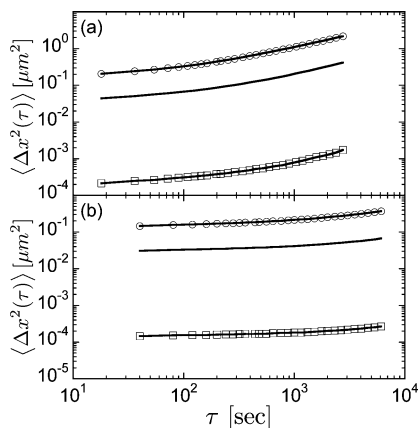


Figure 3. Mean-square displacements, $\langle \Delta x^2(\tau) \rangle$, as a function of lag time, τ , for (a) $\phi = 0.54$ and (b) $\phi = 0.58$ samples of the harder potential. Solid line, sample-averaged $\langle \Delta x^2(\tau) \rangle$; circles, $\langle \Delta x_f^2(\tau) \rangle$ of the particles with displacements in the top 10%; squares, $\langle \Delta x_s^2(\tau) \rangle$ of the particles with displacements in the bottom 10%.

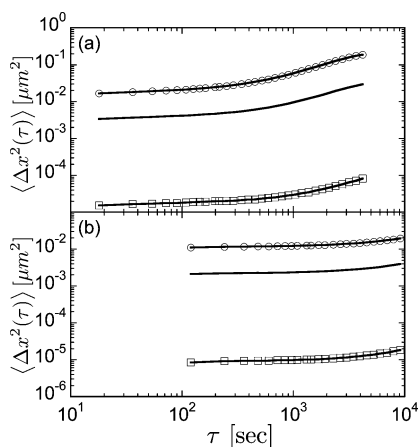


Figure 4. Mean-square displacements, $\langle \Delta x^2(\tau) \rangle$, as a function of lag time, τ , for (a) $\phi = 0.56$ and (b) $\phi = 0.60$ samples of the softer potential. Solid line, sample-averaged $\langle \Delta x^2(\tau) \rangle$; circles, $\langle \Delta x_f^2(\tau) \rangle$ of the particles with displacements in the top 10%; squares, $\langle \Delta x_s^2(\tau) \rangle$ of the particles with displacements in the bottom 10%.

subsets is significantly different. We obtain qualitatively similar results for cutoffs ranging from 5 to 15%.

To probe the relationship between structure and dynamics in our dense suspensions, we then correlate the Voronoi volume to particle displacement for the fastest and slowest subsets, since we expect the correlation to be strongest for those subsets.¹⁸ Such partitioning has been proven to be effective in isolating the properties of mobile and immobile particles.^{19–21} For each time interval, τ , we identify the particles with the 10% largest and smallest displacements over that lag time and calculate the average Voronoi volume of these two subsets of particles. For these calculations, we use the particle's Voronoi volume at the beginning of its displacement; however, using v at any point in the interval τ does not qualitatively change our results. The Voronoi volumes are then normalized by the sample-averaged Voronoi volume, $\langle v \rangle$. We plot the average normalized Voronoi volume of the 10% fastest particles, $\langle \bar{v}_f \rangle = \langle v_f \rangle / \langle v \rangle$, as a function of τ for a supercooled fluid sample of the less-charged colloid preparation at $\phi = 0.54$, where v_f is the Voronoi volume of a fast particle (Figure 5a). $\langle \bar{v}_f \rangle$ increases until $\tau_m \sim 500$ s and then decreases sharply. For comparison, we calculate the cage-rearrangement time scale, τ^* , from the maximum of the non-Gaussian parameter α_2 ; for this sample, $\tau^* \sim 400$ s. The remarkable similarity in time scales for the maximum of $\langle \bar{v}_f \rangle$,

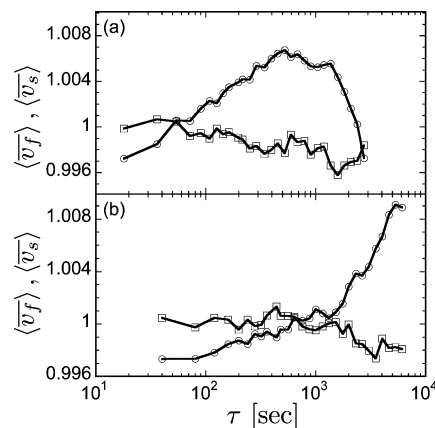


Figure 5. Average Voronoi volume of particles in the harder-potential system with 10% largest (circles, $\langle \bar{v}_f \rangle$) and 10% smallest (squares, $\langle \bar{v}_s \rangle$) displacements at lag time τ for (a) $\phi = 0.54$ and (b) $\phi = 0.58$.

τ_m , and the time scale for maximally non-Gaussian dynamics, τ^* , suggests that a large Voronoi volume is correlated to the large displacements associated with cage breaking. We compare $\langle \bar{v}_f \rangle$ to $\langle \bar{v}_s \rangle$, the average Voronoi volume of the 10% slowest particles, defined similarly. At the shortest measured τ , $\langle \bar{v}_f \rangle$ and $\langle \bar{v}_s \rangle$ are indistinguishable within statistical errors; however, in contrast to $\langle \bar{v}_f \rangle$, $\langle \bar{v}_s \rangle$ decreases slightly with increasing τ .

The Voronoi volume is a measure of the effective local volume fraction, $\phi_{\text{local}} = v_0 / \langle v \rangle$, where v_0 is the volume of a single colloid. The maximum measured difference between $\langle \bar{v}_f \rangle$ and $\langle \bar{v}_s \rangle$ translates into a difference in effective local volume fraction of $\Delta\phi \sim 0.005$. This difference, while small in absolute terms, strongly impacts the relative mobilities of the two dynamical subsets, since even a small change in the effective ϕ can lead to a large change in the local diffusion coefficient when $\phi < \phi_g$.

We observe similar trends in a sample with a higher ϕ , closer to ϕ_g . We plot the normalized average Voronoi volume of the 10% fastest and slowest particles, $\langle \bar{v}_f \rangle$ and $\langle \bar{v}_s \rangle$, versus τ in a sample with $\phi = 0.58$ (Figure 5b). The differences between $\langle \bar{v}_f \rangle$ and $\langle \bar{v}_s \rangle$ are indistinguishable out to $\tau \sim 1000$ s, reflecting the dramatically slowed dynamics. At the longest time scales measured where our statistics are the worst, $\tau \sim 4000$ seconds, we observe a sharp rise in $\langle \bar{v}_f \rangle$ and a slight decline in $\langle \bar{v}_s \rangle$, although we do not observe a rise in the sample-averaged $\langle \Delta x^2(\tau) \rangle$ at these time scales. As in the suspension with $\phi = 0.54$, the cage-rearrangement time scale for this sample, $\tau^* \sim 1000$ s, is of comparable magnitude to the time scale of maximum separation between $\langle \bar{v}_f \rangle$ and $\langle \bar{v}_s \rangle$, $\tau_m \sim 4000$ s.

Our measurements suggest that the average Voronoi volumes of large-displacement particles are slightly larger than those of small-displacement particles, particularly on time scales comparable to or somewhat larger than the cage-rearrangement time scale, τ^* . However, the averages of the Voronoi volumes do not reflect their distributions; in particular, to understand whether Voronoi volume can be used as a predictor of dynamics, we must also examine the distributions of Voronoi volume for the large-displacement and small-displacement particles. We plot $P_*(\bar{v}_f)$ and $P_*(\bar{v}_s)$, the histograms of normalized Voronoi volumes for the 10% fastest and slowest subsets at the cage-rearrangement time scale $\tau^* = 400$ s, for a sample with $\phi = 0.54$ (Figure 6a); at this time scale, the distribution of displacements is highly heterogeneous.^{19,25,26} Although

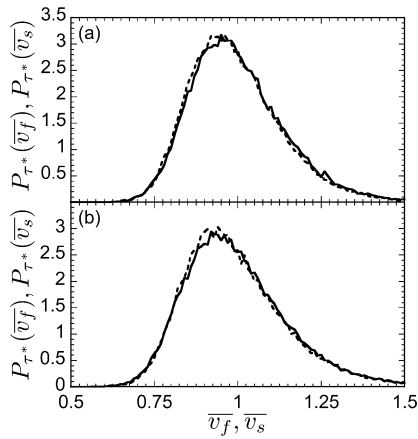


Figure 6. Histogram of Voronoi volumes of particles in the harder-potential system with 10% largest (solid line, $P_*(v_f)$) and 10% smallest (dotted line, $P_*(v_s)$) displacements at the relaxation time Δt^* : (a) $\phi = 0.54$, $\Delta t^* = 400$ s; (b) $\phi = 0.58$, $\Delta t^* = 2000$ s.

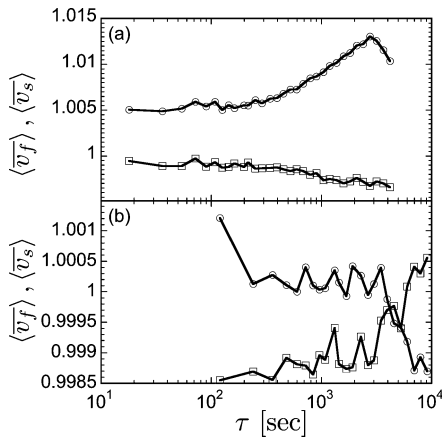


Figure 7. Average Voronoi volume of particles in the softer-potential system with 10% largest (circles, $\langle v_f \rangle$) and 10% smallest (squares, $\langle v_s \rangle$) displacements at lag time τ for (a) $\phi = 0.56$ and (b) $\phi = 0.60$.

$\bar{v}_f \geq \bar{v}_s$, $P_*(\bar{v}_f)$ and $P_*(\bar{v}_s)$ are nearly identical; however, $P_*(\bar{v}_f)$ is shifted almost imperceptibly to higher volumes. The histograms of small- and large-displacement Voronoi volumes for the denser supercooled fluid at $\phi = 0.58$ plotted at $\tau^* = 2000$ s are also nearly identical (Figure 6b). \bar{v}_f and \bar{v}_s are distinct, with a difference that reflects a measurable reduction in local volume fraction for the large-displacement particles. However, this difference is small in absolute terms, so that the distributions $P_*(\bar{v}_f)$ and $P_*(\bar{v}_s)$ are nearly identical, even on the time scale of greatest dynamical heterogeneity. Therefore, although weak trends exist between Voronoi volume and displacement, for this particular colloidal preparation, the Voronoi volume is not a strong predictor of dynamical behavior.

For the other colloidal preparation with a slightly softer potential, the Voronoi distributions do not collapse to a universal form. To test whether the difference in structure leads to a measurable difference in the dynamics, we correlate Voronoi volume to displacement in the softer-potential suspension. We plot $\langle v_f \rangle$ for a sample of the softer-potential colloidal preparation with $\phi = 0.56 < \phi_g$ (Figure 7a). As also observed in the less-charged colloid preparation, $\langle v_f \rangle$ increases with increasing time and has a maximum at $\tau \sim 3000$ s; τ_m is again remarkably similar to the cage-rearrangement time scale, $\tau^* = 1000$ s. The behavior of $\langle v_s \rangle$ is similar to that of the other preparation; at short times, $\langle v_f \rangle \geq \langle v_s \rangle$ and $\langle v_s \rangle$ decreases with increasing τ .

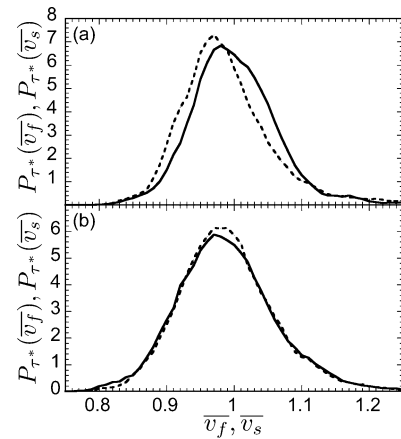


Figure 8. Histogram of Voronoi volumes of particles in the softer-potential system with 10% largest (solid line, $P_*(v_f)$) and 10% smallest (dotted line, $P_*(v_s)$) displacements at the relaxation time Δt^* : (a) $\phi = 0.56$, $\Delta t^* = 1000$ s; (b) $\phi = 0.60$, $\Delta t^* = 3000$ s, in the system with softer potential.

The maximum difference between $\langle v_f \rangle$ and $\langle v_s \rangle$ for this suspension is greater than that observed in any sample from the other, harder-potential preparation. The maximum difference between the local ϕ of the large- and small-displacement particles is $\Delta\phi \sim 0.009$, again showing that the local cage of the large-displacement particles is slightly larger than that of the small-displacement particles. Although the static distributions of Voronoi volume of the two colloidal preparations differ, we observe qualitatively similar behavior of $\langle v_f \rangle$ and $\langle v_s \rangle$ in both preparations.

Finally, for comparison, we also plot $\langle v_f \rangle$ and $\langle v_s \rangle$ for a colloidal glass sample with $\phi = 0.60$ (Figure 7b). We observe that $\langle v_f \rangle$ and $\langle v_s \rangle$ are not distinguishable to within statistical error at all measured lag times; this resembles the short-time behavior of the other suspensions.

To test the predictive power of Voronoi volume in the softer-potential preparation, we plot the histograms of Voronoi volumes, $P_*(v_s)$ and $P_*(v_f)$, for the slowest and fastest particles at the cage-rearrangement time scale $\tau^* = 1000$ s at $\phi = 0.56$ (Figure 8a), on which the dynamics are most heterogeneous. The difference between the distributions is the largest measured in all experiments but is nevertheless still small. In contrast, the histograms of the slowest and fastest particles for a glass sample above the glass transition, $\phi = 0.60$, overlap completely (Figure 8b). Although the widths of the softer-potential distributions are generally smaller, the distributions for the softer-potential preparation qualitatively resemble those from the harder-potential preparation. These results again confirm that Voronoi volume is not a good predictor of dynamics in colloids.

While the trend of weak correlation between volume and displacement observed in our measurements is robust for all ϕ of both preparations, there are both spatial and temporal limitations to our experimental resolution. The minimum resolvable displacement in our experiments is roughly $0.06 \mu\text{m}$. The typical displacement of a particle in the bottom 10% is somewhat smaller than this; for example, a particle in the bottom 10% of the $\phi = 0.58$ sample has a displacement at $\tau \sim 1000$ s of $0.003 \mu\text{m}$, significantly below our spatial resolution threshold. Therefore, in these experiments, we are unable to distinguish particles with displacements in the bottom 10% from those in the bottom 50%. This lack of resolution may distort our correlations between displacement and Voronoi volume; we cannot precisely ascertain from these measurements the particles

that have the smallest displacements. Other criteria for identifying static particles^{27–29} may be more effective at identifying the most glasslike particles. Besides the limited spatial resolution, our measurements also have limited temporal resolution. A typical three-dimensional stack of confocal images takes roughly 10 s to acquire; therefore, we cannot probe the very short time scales where the correlations between local volume and displacement may be the strongest.

4. Simulation Results

While limitations on resolution exist, we nevertheless believe that the robust trends found in the experimental data are valid. To further evidence the lack of correlation between Voronoi volume and dynamics, we compare our results to those from molecular-dynamics simulations of a polymer melt containing 100 chains of “bead-spring” polymers.⁶ Each chain consists of 20 monomers interacting via a Lennard-Jones (LJ) potential

$$V_{\text{LJ}} = 4\epsilon \left[\left(\frac{\sigma}{r} \right)^{12} - \left(\frac{\sigma}{r} \right)^6 \right]$$

where r is the distance between monomers, σ is the monomer size, and ϵ is the strength of the interaction. The LJ potential is truncated so that both the potential and force continuously go to zero at a distance of 2.5σ . Neighboring monomers along a chain also interact via a finitely extensible nonlinear elastic (FENE) spring potential.

$$V_{\text{FENE}} = -k(R_0^2/2) \ln(1 - (r/R_0)^2)$$

To study glass formation in this model system, we use the parameters $k = 30\epsilon$ and $R_0 = 1.5\sigma$, which are known to avoid crystallization.^{30,31}

To compare with the previous experiments, we examine a state point at $T = 0.35$ and $\rho = 1.0$; temperature is measured in “reduced units” of ϵ/k_B , and density is expressed in term of σ^{-3} . The mode-coupling temperature at this density for this system is $T_{\text{MCT}} = 0.35 \pm 0.01$. Typically, $T_{\text{MCT}} \approx 1.2T_g$, cold enough that the dynamics are highly heterogeneous at intermediate time scales, but relaxation still occurs on a time scale that makes equilibrium simulations possible. The Voronoi volume distributions for this system are known to collapse onto a universal master curve.⁶

We plot the normalized average Voronoi volume of the 10% particles with the largest and smallest displacements for a simulation run at $T = 0.35$ in Figure 9a; the time axis has been normalized by the time τ^* where α_2 has a maximum. The qualitative trends observed in experiment are also observed in the simulations. The time scale of the maximum of $\langle \bar{v}_i \rangle$, $\tau_m \approx 0.1$, is slightly smaller than but comparable to the cage-rearrangement time scale, $\tau^* = 1$. The maximum separation between $\langle \bar{v}_i \rangle$ and $\langle \bar{v}_s \rangle$ is approximately 0.03, somewhat greater than that observed in experiment. The histogram of the Voronoi volumes of the 10% fastest and slowest particles at τ^* , plotted in Figure 9b, again qualitatively resemble the colloid results; the distributions overlap significantly, with small separation observed between the two peaks. These simulation results strongly support the experimental conclusion that Voronoi volume and dynamic properties are only weakly correlated, even in thermal systems.

We also investigate the unexpected lack of scaling of the Voronoi volume distributions for the softer-core colloids with simulation. To probe the origin of this breakdown of the scaling, we first simulate a system of monomers interacting via

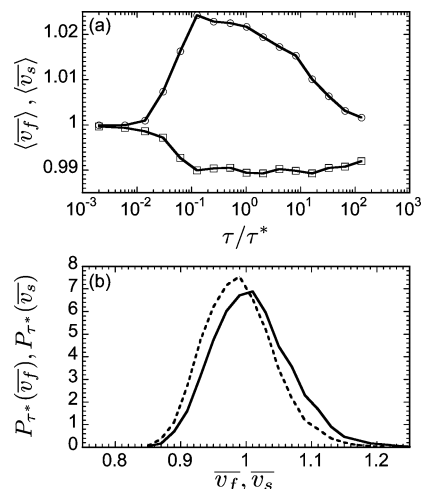


Figure 9. Results from molecular-dynamics simulation of polymer chains: (a) average Voronoi volume of monomers with 10% largest (circles, $\langle \bar{v}_i \rangle$) and 10% smallest (squares, $\langle \bar{v}_s \rangle$) displacements at lag time τ for simulated polymer chains at $T = 0.35$; (b) histogram of Voronoi volumes of monomers with 10% largest (circles, $P_*(\bar{v}_i)$) and 10% smallest (squares, $P_*(\bar{v}_s)$) displacements at the cage-rearrangement time $\tau^* = 73$ and at $T = 0.35$.

$V_{\text{soft}} = \epsilon(\sigma/r)^3$. This core repulsion is far weaker than that of the LJ potential, or of any realistic liquid system. We calculate $P(v)$ for eight densities in the range $0.8 < \rho < 1.5$ at $T = 1$ and find that the distribution $P(v)$ scales as expected. The observation of scaling in this softer-core potential suggests that the scaling breakdown observed in our colloids is not simply due to the soft-core potential.

The softer-core colloids also are more strongly charged, leading to long-ranged interactions. To determine whether this long-ranged repulsion is the origin of the deviations from scaling, we also simulate a model for charged colloids³² that includes a long-ranged repulsive Yukawa interaction of the form $V_Y = Ae^{-r/\xi}/(r/\xi)$, where $A = 0.05$ is the strength of repulsion and $\xi = 2$ is the range. We simulate this model at a density of 0.942 and again find that $P(v)$ scales to the expected universal form.

The origin of the breakdown of scaling in the experimental system is puzzling, since scaling is observed in both the soft-core and long-ranged repulsive systems in simulation. The anisotropy of the core interactions of the colloids may perhaps influence the scaling behavior. However, even highly anisotropic liquids, such as water and silica, conform to the universal distribution.⁶ To determine the source of the breakdown in scaling, further investigation of the soft-core experimental system is required.

5. Conclusions

In experiments on dense colloidal suspensions imaged by confocal microscopy, we have investigated the relationship between local structure, as characterized by a particle’s Voronoi volume, and local dynamics, as characterized by a particle’s displacement, in two different colloidal preparations. The distribution of Voronoi volumes is universal for one preparation and nonuniversal for the other. Furthermore, in both preparations, the correlation between Voronoi volume and displacement is weak, although the correlations are most pronounced in the preparation with a harder interparticle potential below ϕ_g . The maximum correlation between Voronoi volume and displacement occurs at a time scale comparable to the cage-rearrangement time scale. While our temporal and spatial resolution may

limit our ability to detect this correlation, even in molecular-dynamics simulations, the calculated correlations between Voronoi volume and displacement are small. Our measurements of the weak correlations between Voronoi volume and displacement in colloidal suspensions suggest that testing free volume ideas in these systems will be difficult, since the differences in volume between mobile and immobile particles are small. The changes in local free volume may be so small for colloidal systems that correlating the free volume to displacement on the scale of a single particle does not reveal significant correlation. Ultimately, a different approach to testing free volume ideas is necessary. For example, more pronounced correlations may be observed after coarse-graining. Alternatively, it may be necessary to consider the effective free volume of particles correlated over a larger region in space, reflecting the collective motion of the structural relaxation.

Acknowledgment. J.C.C. and D.A.W. acknowledge support from the NSF [DMR-0243715] and the Harvard University MRSEC [DMR-0213805]. This paper is dedicated to our friend and colleague, Irwin Oppenheim.

References and Notes

- (1) Cohen, M. H.; Turnbull, D. *J. Chem. Phys.* **1959**, *31*, 1164.
- (2) Turnbull, D.; Cohen, M. H. *J. Chem. Phys.* **1961**, *34*, 120.
- (3) Turnbull, D.; Cohen, M. H. *J. Chem. Phys.* **1970**, *52*, 4048.
- (4) Cohen, M. H.; Grest, G. S. *Phys. Rev. B* **1979**, *20*, 1077.
- (5) Rahman, A. *J. Chem. Phys.* **1966**, *45*, 2585.
- (6) Starr, F. W.; Sastry, S.; Douglas, J. F.; Glotzer, S. C. *Phys. Rev. Lett.* **2002**, *89*, 125501.
- (7) Percus, J. K.; Yeveick, G. J. *Phys. Rev.* **1958**, *110*, 1.
- (8) Bernal, J. D. *Nature* **1959**, *183*, 141.
- (9) Chandler, D.; Weeks, J. D.; Andersen, H. C. *Science* **1983**, *220*, 787.
- (10) Medvedev, N. N.; Geiger, A.; Brostow, W. *J. Chem. Phys.* **1990**, *93*, 8337.
- (11) Voloshin, V. P.; Naberukhin, Y. I.; Medvedev, N. N.; Jhon, M. S. *J. Chem. Phys.* **1995**, *102*, 4981.
- (12) Hiwatari, Y. *J. Chem. Phys.* **1982**, *76*, 5502.
- (13) Hiwatari, Y.; Saito, T.; Ueda, A. *J. Chem. Phys.* **1984**, *81*, 6044.
- (14) Kegel, W. K.; van Blaaderen, A. *Science* **2000**, *287*, 290.
- (15) Weeks, E. R.; Crocker, J. C.; Levitt, A. C.; Schofield, A.; Weitz, D. A. *Science* **2000**, *287*, 627.
- (16) Gasser, U.; Weeks, E. R.; Schofield, A.; Pusey, P. N.; Weitz, D. A. *Science* **2001**, *292*, 256.
- (17) Dinsmore, A. D.; Weeks, E. R.; Prasad, V.; Levitt, A. C.; Weitz, D. A. *Appl. Opt.* **2001**, *40*, 4152.
- (18) Weeks, E. R.; Weitz, D. A. *Phys. Rev. Lett.* **2002**, *89*, 95704.
- (19) Kob, W.; Donati, C.; Plimpton, S. J.; Poole, P. H.; Glotzer, S. C. *Phys. Rev. Lett.* **1997**, *79*, 2827.
- (20) Donati, C.; Douglas, J. F.; Kob, W.; Plimpton, S. J.; Poole, P. H.; Glotzer, S. C. *Phys. Rev. Lett.* **1998**, *80*, 2338.
- (21) Donati, C.; Glotzer, S. C.; Poole, P. H.; Kob, W.; Plimpton, S. J. *Phys. Rev. E* **1999**, *60*, 3107.
- (22) Antl, L.; Goodwin, J. W.; Hill, R. D.; Ottewill, R. H.; Owens, S. M.; Papworth, S.; Waters, J. A. *Colloids Surf.* **1986**, *17*, 67.
- (23) Crocker, J. C.; Grier, D. G. *J. Colloid Interface Sci.* **1996**, *179*, 298.
- (24) Qhull code for Convex Hull, Delaunay Triangulation, Voronoi Diagram, and Halfspace Intersection about a Point, <http://www.qhull.org> (accessed November 2002).
- (25) Kasper, A.; Bartsch, E.; Sillescu, H. *Langmuir* **1998**, *14*, 5004.
- (26) Doliwa, B.; Heuer, A. *J. Phys.: Condens. Matter* **1999**, *11*, A277.
- (27) Rabani, E.; Gezelter, J. D.; Berne, B. J. *J. Chem. Phys.* **1997**, *107*, 6867.
- (28) Rabani, E.; Gezelter, J. D.; Berne, B. J. *Phys. Rev. Lett.* **1999**, *82*, 3649.
- (29) Doliwa, B.; Heuer, A. *J. Non-Cryst. Solids* **2002**, *307*, 32.
- (30) Bennemann, C.; Baschnagel, J.; Paul, W. *Eur. Phys. J. B* **1999**, *10*, 323.
- (31) Bennemann, C.; Donati, C.; Baschnagel, J.; Glotzer, S. C. *Nature* **1999**, *399*, 246.
- (32) Sciortino, F.; Mossa, S.; Zaccarelli, E.; Tartaglia, P. *Phys. Rev. Lett.* **2004**, *93*, 055701.